Current Research in Toxicology 1 (2020) 56–69

Contents lists available at ScienceDirect

Current Research in Toxicology

journal homepage: www.elsevier.com/locate/crtox

Comparison of the basic morphology and function of 3D lung epithelial cultures derived from several donors

David Bovard *,[1], Albert Giralt [1], Keyur Trivedi, Laurent Neau, Petros Kanellos, Anita Iskandar, Athanasios Kondylis, Karsta Luettich, Stefan Frentzel, Julia Hoeng, Manuel C. Peitsch

PMI R&D, Philip Morris Products S.A., Quai Jeanrenaud 5, 2000 Neuchâtel, Switzerland

ARTICLE INFO

Article history:
Received 2 June 2020
Received in revised form 25 August 2020
Accepted 27 August 2020

ABSTRACT

In vitro models of the human lung play an essential role in evaluating the toxicity of inhaled compounds and understanding the development of respiratory diseases. Three-dimensional (3D) organotypic models derived from lung basal epithelial cells and grown at the air–liquid interface resemble human airway epithelium in multiple aspects, including morphology, cell composition, transcriptional profile, and xenobiotic metabolism. Whether the different characteristics of basal cell donors have an impact on model characteristics and responses remains unknown. In addition, studies are often conducted with 3D cultures from one donor, assuming a representative response on the population level. Whether this assumption is correct requires further investigation. In this study, we compared the morphology and functionality of 3D organotypic bronchial and small airway cultures from different donors at different weeks after air-lift to assess the interdonor variability in these parameters. The thickness, cell type composition, and transepithelial electrical resistance varied among the donors and over time after air-lift. Cilia beating frequency increased in response to isoproterenol treatment in both culture types, independent of the donor. The cultures presented low basal cytochrome P450 (CYP) 1A1/1B1 activity, but 2,3,7,8-tetrachlorodibenzo-p-dioxin (TCDD) treatment induced CYP1A1/1B1 activity regardless of the donor. In conclusion, lung epithelial cultures prepared from different donors present diverse morphology but similar functionality and metabolic activity, with certain variability in their response to stimulation.

1. Introduction

The respiratory system is an essential organ system that is in direct and constant contact with the environment through air exposure. Inhalation toxicology is a priority area for many governmental organizations, and in vitro human lung models play an essential role in evaluating the toxicity of aerosols and in mimicking respiratory diseases. Like other in vitro models, lung models have recently benefited from major advances in cell culture technologies, progressively moving away from cells cultured in 2 dimensions toward fully differentiated 3D tissues, which mimic more closely the in vivo situation.

One of the most common approaches for preparing 3D lung models involves seeding human primary lung basal epithelial cells on top of a microporous membrane and exposing them to air on their apical side (a step called “air-lift”) to trigger basal cell differentiation. After 3 to 4 weeks at the air–liquid interface (ALI), the cells typically form a pseudostratified epithelium composed of secretory, ciliated, and basal cells (Gray et al., 1996; Karp et al., 2002). Lung epithelial cells grown at the ALI recapitulate the human airway epithelium in multiple aspects, including morphology, cell type composition, transcriptional profile, and xenobiotic metabolism (Karp et al., 2002; Baxter et al., 2015; Pezzulo et al., 2011). Nasal (Müller et al., 2013), bronchial (Karp et al., 2002), and small airway epithelial cultures (Huang et al., 2017) have been generated by following similar methods by using basal cells from the corresponding respiratory compartments. Because they allow direct exposure to aerosols on the apical side, these 3D ALI models were previously used to assess the biological effects of aerosols (e.g., cigarette smoke (Czekala et al., 2019; Iskandar et al., 2017a; Iskandar et al., 2018), air pollutants (Ghio et al., 2013), and airborne particles (Ji et al., 2017; Wilkinson et al., 2011)) or study lung pathologies in vitro (e.g., asthma (Hackett et al., 2011), chronic obstructive pulmonary disease (Schneider et al., 2010), and cystic fibrosis (Tarran et al., 2005)).

Sex, age, and ethnicity have been shown to impact the incidence, susceptibility, and severity of several lung diseases (Braun et al., 2013; Carey et al., 2007; Meiners et al., 2015). Thus, investigating whether 3D lung cultures derived from different donors present different characteristics and show different responses to certain stimuli is important. In addition, a

Abbreviations: ALI, air–liquid interface; BTUB4, β-tubulin 4; CBF, cilia beating frequency; CYP, cytochrome P450; MUC5AC, mucin 5AC; PBS, phosphate buffered saline; TCDD, 2,3,7,8-tetrachlorodibenzo-p-dioxin; TEER, transepithelial electrical resistance.

* Corresponding author at: Quai Jeanrenaud 5, 2000 Neuchâtel, Switzerland.
E-mail address: david.bovard@pmi.com. (D. Bovard).

[1] These authors contributed equally to the manuscript.

http://dx.doi.org/10.1016/j.crtox.2020.08.002

better understanding of the potential donor effect(s) on tissue characteristics could lead to a better estimation of interdonor variability, guide decisions toward more appropriate experimental designs (including an appropriate number of donors), and ultimately yield more robust data in support of Integrated Approaches to Testing and Assessment. Here, we evaluated the influence of the donor on the characteristics of 3D lung epithelial cultures differentiated at the ALI. We investigated the impact of the donor of the basal cells on the morphology (histological and whole-insert immunostaining characteristics), functionality (transepithelial electrical resistance [TEER] and cilia beating frequency [CBF] measurements), and metabolic capacity (cytochrome P450 [CYP] 1A1/1B1 enzymatic activity) of human 3D bronchial epithelial cultures prepared in-house and of commercially available human 3D small airway epithelial cultures (SmallAir™, Epithelix, Geneva, Switzerland) over several weeks in culture.

2. Materials and methods

2.1. Human 3D bronchial epithelial cultures

We prepared human 3D bronchial epithelial cell cultures as previously described (Bovard et al., 2018). Briefly, primary normal human bronchial epithelial (NHBE) cells (Lonza, Basel, Switzerland) from 5 different donors (Table 1) were first cultured in PneumaCult-Ex Plus™ medium (STEMCELL Technologies, Vancouver, Canada) at 37 °C with 5% CO_2 and 90% relative humidity. Once the cells were approximately 80% confluent, they were detached from the flask by using trypsin–EDTA (ethylenediaminetetraacetic acid; Lonza), and 50,000 cells were seeded on a 6.5-mm-diameter collagen I-coated Transwell® insert with 0.4-μm pore size (Corning®, Corning, NY, USA). Both the apical and basal sides of the inserts were filled with PneumaCult-Ex Plus™ medium, and the cells were incubated for 3 days. Subsequently, the cells were air-lifted by removing the apical medium; the basal medium was replaced with PneumaCult™-ALI medium (STEMCELL Technologies), which was renewed every 2 or 3 days. The cultures were considered mature after 4 weeks at the ALI and used for experiments at weeks 5, 7, and 9 after air-lift.

2.2. Human 3D small airway epithelial cultures

SmallAir™ cultures (Epithelix) are 3D lung epithelial cultures reconstituted from primary human small airway epithelial cells isolated from the distal lung compartment and grown in a 6.5-mm Transwell® insert with a 0.4-μm pore size polyester membrane (Corning®) (Huang et al., 2017). For the present study, we used SmallAir™ cultures from 6 different donors (Table 1). Upon receipt, the cultures were maintained in the medium provided by the supplier (SmallAir™ medium, Epithelix) and cultured at 37 °C with 5% CO_2 and 90% relative humidity. The basal medium was changed every 3 days, and the apical surface of the cultures was rinsed once every week with culture medium. The tissues were used for experiments during 4 consecutive weeks (weeks 8 to 11 after air-lift).

2.3. Histological processing

At weeks 5, 7, and 9 after air-lift of the bronchial cultures or weeks 8 and 11 after air-lift of the small airway cultures, the cultures were washed apically and basolaterally 3 times with phosphate-buffered saline (PBS) (Merck, Darmstadt, Germany) and fixed for 2 h in a ready-to-use 4% (*w/v*) paraformaldehyde solution in PBS (Thermo Fisher Scientific, Waltham, MA, USA). After fixation, the cultures were washed 3 times in PBS and bisected at the midpoint. The 2 bisected pieces were placed in cassettes and processed with the Leica ASP300 S Tissue Processor (Leica Biosystems Nussloch GmbH, Nussloch, Germany). The processed cultures were embedded vertically and in parallel by using the MEDITE TES Valida Tissue Embedding System (MEDITE GmbH, Burgdorf, Germany), and 5-μm-thick sections were cut by using a Leica RM2255 microtome (Leica Biosystems Nussloch GmbH). The cut sections were mounted on Superfrost™ Plus slides (Thermo Fisher Scientific) and transferred to the Leica ST5020 automated stainer (Leica Biosystems Nussloch GmbH) for staining with hematoxylin, eosin, and Alcian blue. The stained slides were covered with coverslips automatically by using the Leica CV5030 automated coverslipper (Leica Biosystems Nussloch GmbH). Digital images of the stained slides were generated by using the NanoZoomer 2.0 slide scanner (Hamamatsu Photonics, Hamamatsu, Japan) at 40× magnification. The generated digital images were used to measure epithelium thickness in different regions of the tissue (border and center) by using the NDP.view2 software (Version 2.7.25, Hamamatsu Photonics).

2.4. Immunohistochemical analysis

Automated immunohistochemical analysis was performed with the Leica BOND-MAX system (Leica Biosystem Nussloch GmbH) by using a Leica BOND Polymer Refine Detection kit for anti-CC10 (Clone E11, Santa Cruz Biotechnologies, Inc., Santa Cruz, CA, USA) and anti-MUC5AC (AM32160PU-N, ACRIS Antibodies GmbH, Herford, Germany) primary antibodies. After staining, the slides were washed, dehydrated, and coverslipped by using the Leica CV5030 automated coverslipper (Leica Biosystems Nussloch GmbH). Digital images were generated by using the NanoZoomer 2.0 slide scanner (Hamamatsu Photonics, Hamamatsu, Japan).

2.5. Whole-insert immunostaining

To detect the goblet and ciliated cells present in the cultures, antibodies were used to target specific cell type markers. Each culture was first fixed in 4% paraformaldehyde (Thermo Fisher Scientific) for 15 min and then blocked for 1 h in a blocking solution (0.5% Triton™ X-100 [Thermo Fisher Scientific], 5% normal goat serum [Thermo Fisher Scientific], and 2% bovine serum albumin [Thermo Fisher Scientific] in PBS). The cultures were stained with a β-tubulin 4 antibody (BTUB4; ciliated cell marker) conjugated to Alexa 647 (clone EPR16775, Abcam, Cambridge, United Kingdom) or a MUC5AC antibody (goblet cell marker) conjugated to Alexa 555 (clone EPR16904, Abcam), diluted in PBS with 2% normal

Table 1
Characteristics of the cell donors.

Culture type	Donor ID	Donor number	Age	Sex	Ethnicity	Smoking status	Supplier
Bronchial	BR1	28607	30	Male	Hispanic	Smoker	Lonza
Bronchial	BR2	28968	38	Male	Caucasian	Nonsmoker	Lonza
Bronchial	BR3	32134	60	Male	Black	Unknown	Lonza
Bronchial	BR4	32254	19	Female	Black	Unknown	Lonza
Bronchial	BR5	33652	56	Male	Black	Nonsmoker	Lonza
Small airway	SA1	SA0664	28	Male	Caucasian	Smoker	Epithelix
Small airway	SA2	SA0671	72	Male	Caucasian	Nonsmoker	Epithelix
Small airway	SA3	SA0529	72	Male	Caucasian	Nonsmoker	Epithelix
Small airway	SA4	SA0610	47	Female	Caucasian	Nonsmoker	Epithelix
Small airway	SA5	SA0685	48	Female	Caucasian	Smoker	Epithelix
Small airway	SA6	SA0665	55	Female	Caucasian	Nonsmoker	Epithelix

goat serum and 1% bovine serum albumin. Finally, nuclei were counterstained with Hoechst 33342 dye (Thermo Fisher Scientific). For these MUC5AC- and BTUB4-stained slides, 4 and 16 contiguous fields of view located at the center of the inserts (see Fig. S1) were acquired, respectively. Images were acquired with the CellInsight™ CX7 high-content screening platform (Thermo Fisher Scientific), and positively stained cells were quantified as previously described (Marescotti et al., 2020).

2.6. TEER measurement

TEER was measured longitudinally in 4 bronchial cultures at weeks 5, 7, and 9 after air-lift and in 3 small airway cultures at weeks 8, 9, 10, and 11 after air-lift. TEER was measured by using an EndOhm-6 chamber (WPI, Sarasota, FL, USA) connected to an EVOM™ Epithelial Voltohmmeter (WPI) in accordance with the manufacturer's instructions. The value obtained with an empty insert was subtracted from the value displayed by the voltohmmeter with an insert containing a tissue and multiplied by the surface of the insert (0.33 cm^2) to obtain the resistance value in the total area (Ohm x cm^2).

2.7. CBF measurement

CBF was measured by using an inverted microscope (Zeiss, Oberkochen, Germany) equipped with a 4× objective and a 37 °C chamber and connected to a high-speed camera (Basler AG, Ahrensburg, Germany). Short movies composed of 512 frames recorded at 120 images per second were analyzed by using the SAVA analysis software (Ammons Engineering, Clio, MI, USA). CBF was measured longitudinally in 4 bronchial cultures at weeks 5, 7, and 9 and in 3 small airway cultures at weeks 8, 9, 10, and 11 after air-lift. CBF was measured first at steady state and then after a 30-min treatment with 100 μM isoproterenol (Merck, Darmstadt, Germany) diluted in the respective cell culture medium.

2.8. Measurement of CYP enzymatic activity

CYP1A1/1B1 enzyme (combined) activity was measured longitudinally in the same 4 bronchial cultures per condition (i.e., basal state and induced state) at weeks 5, 7, and 9 after air-lift and in the same 3 small airway cultures per condition at weeks 8, 9, 10, and 11 after air-lift. CYP1A1/1B1 activity was measured by using the P450-Glo™ kit (Promega, Madison, WI, USA) in accordance with the manufacturer's protocol. To induce CYP1A1/1B1 activity, the cultures were incubated with 10 nM 2,3,7,8-tetrachlorodibenzo-p-dioxin (TCDD; Merck, Darmstadt, Germany) for 48 h at each time point. TCDD treatment was renewed 24 h after the first exposure.

2.9. Statistical analysis and data repository

A variance component estimation was performed to estimate the relative contribution of the donor of origin to the variance in the endpoints analyzed (TEER, CBF, and CYP1A1/1B1 activity). The components of variance were calculated by restricted maximum likelihood estimation through the random effects summary of the “lme” function in the R-package “lme4”. Negative and positive controls—such as isoproterenol-treated cultures for CBF measurement or TCDD-treated cultures for enzyme activity measurement—as well as time after air-lift were considered fixed experimental factors. Donor and experimental week were considered random effects. The results of the variance component estimation are provided in relative terms (as a percentage of the total variance).

Datasets, further details on the protocols, and additional data visualizations are available on the INTERVALS platform at https://doi.org/10.26126/intervals.5g6f4t.1.

3. Results

3.1. Morphological characterization of bronchial cultures from 5 different donors

The bronchial barrier in vivo is a pseudostratified epithelium composed of at least 3 different cell types: basal, goblet, and ciliated cells. In the present study, human NHBE cells from 5 different donors (Table 1) were used. Histological analysis of 3 bronchial cultures per donor was performed at weeks 5, 7, and 9 after air-lift. At week 5, the bronchial cultures presented a thickness ranging from 40 to 100 μm (Fig. 1), which is similar to the epithelial thickness in human adults (Tsartsali et al., 2011). The thickness and absence/presence of vacuoles (or cysts) varied among the donors. With the exception of donor BR3, most donors presented a thick layer of undifferentiated cells between the differentiated cells and the basal cells residing on the porous membrane (see arrows, Fig. 1). Given the culture thickness and presence of cysts, the cultures prepared with cells from donors BR4 and BR5 were not properly pseudostratified (i.e., the tissues were very thick, and the differentiated cells were not in contact with the membrane). Cultures prepared with cells from donors BR1, BR2, particularly BR4, and BR5, presented large cysts that produced an irregular surface on the cultures. Generally, these cysts were filled with mucus at week 5, but mucus was not apparent at week 9 in any culture. The cysts were also lined with ciliated and goblet cells oriented inward at week 9 (forming a pseudo-ALI).

Ciliation and presence of goblet cells in the bronchial cultures were evaluated by using an antibody-based approach for detecting these 2 cell populations by immunofluorescence. We used a β-tubulin 4 antibody to stain the cilia (Fig. 2) and a high-content screening platform to acquire 16 contiguous fields of view at the center of the insert (representing ~40% of the whole insert surface; Fig. S1). In cultures prepared with cells from donors BR1, BR4, and BR5, ciliation was non-homogeneous, with large regions of the culture surface remaining unstained (although it was less in donors BR1 and BR4). We observed that, in all cultures, ciliation increased over time, which was confirmed by the results of quantification of the total intensity of β-tubulin 4 spots (Fig. 3A). Variance component analysis indicated that ~78% of the variability was caused by the donor (Fig. 3B). The residual and time factors had a small impact on the total variance composition (~8 and ~ 13%, respectively).

The cultures were stained with a MUC5AC antibody to visualize goblet cells (Fig. 4). From these stained cultures, 4 adjacent fields of view at the center of the insert were acquired (representing ~10% of the whole insert surface; Fig. S1). Because of the low number of MUC5AC-positive cells present in each culture and the difficulty in visualizing the antibody staining when Hoechst staining is also visible, Fig. 4 shows only the MUC5AC staining in grey scale, without the stained nuclei. The number of MUC5AC-positive cells increased over time in all cultures, except in those from donors BR1 and BR2, in which the number of MUC5AC-positive cells decreased at week 7 before increasing at week 9 (Fig. 4). At a given time point, the number of goblet cells varied depending on the donor: Donor BR2, for example, exhibited up to 10 times more MUC5AC-positive cells at week 9 than donor BR3 (Fig. 5A). In contrast to the distribution of ciliated cells, goblet cell distribution over the culture surface remained homogeneous over time. Analysis of the composition of variance showed that ~57% of the variance was caused by the donor, ~25% by the time factor, and the rest by residual variability (Fig. 5B).

3.2. Morphological characterization of small airway cultures from 6 different donors

Histological analysis of 3 small airway cultures from each donor was performed at weeks 8 and 11 after air-lift. In general, the small airway cultures were thinner than the bronchial cultures, ranging from 15 to 40 μm, consistent with the in vivo situation (Hastedt et al., 2016) (Fig. 6). At week 8, the cultures from donors SA1, SA5, and SA6 presented a homogenous, columnar pseudostratified epithelium, with the distinct presence of ciliated cells. The cultures obtained from donor SA2 also showed a fully differentiated columnar epithelium, but they were thicker than the cultures

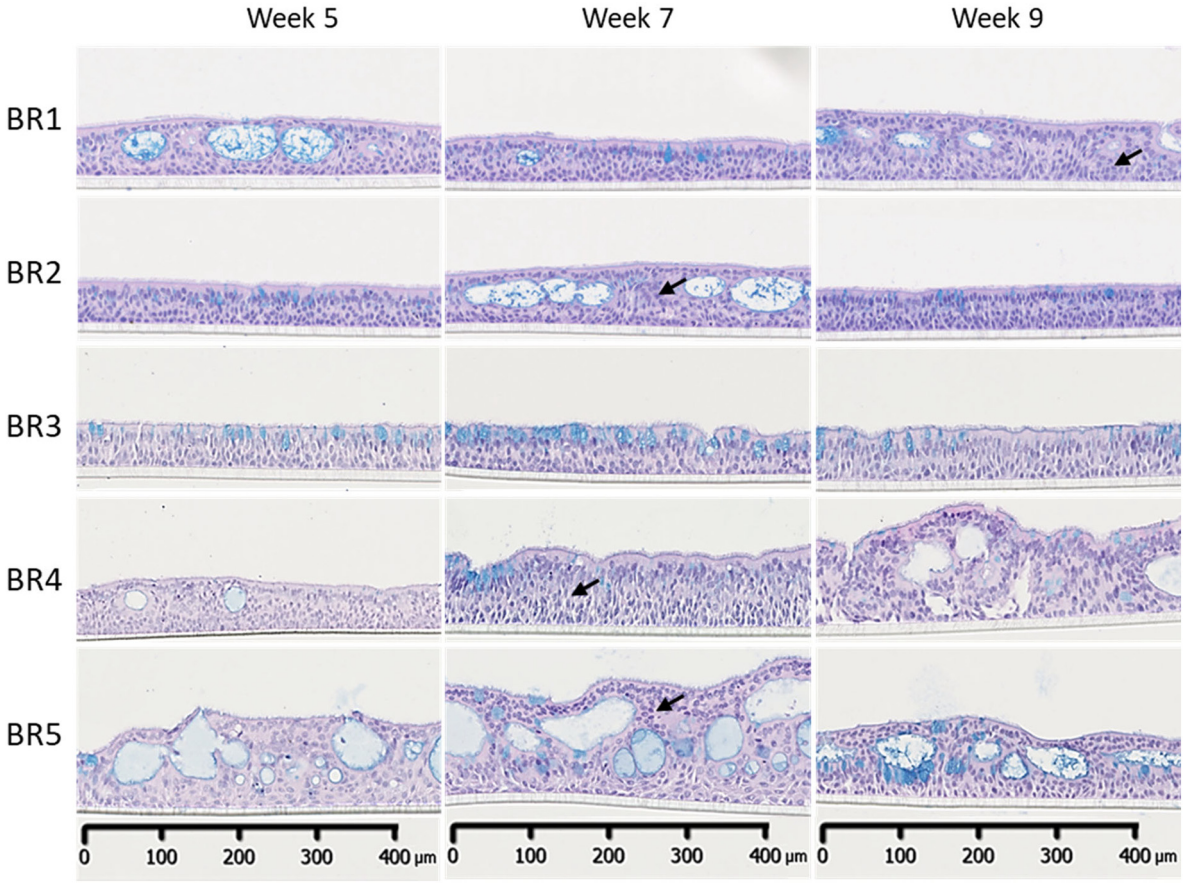

Fig. 1. Representative histological sections of bronchial cultures at weeks 5, 7, and 9 after air-lift. Representative images of bronchial culture sections stained with hematoxylin, eosin, and Alcian blue from samples collected 5, 7, and 9 weeks after air-lift. Three technical replicates were used for histological analysis per time point. Black arrows show the non-differentiated cells located between the differentiated and basal cells. Magnification: 20×.

from the other donors and were the only small airway cultures that showed the presence of cysts. In contrast, the cultures from donors SA3 and SA4 presented a thinner epithelium, but the epithelium was not homogenous, with some areas being particularly thin. The cultures from donors SA3 and SA4 also presented higher volumes of apical surface liquid than those from the other donors (visually assessed; data not shown). At the end of the experimental period (week 11 after air-lift), the epithelium thickness had decreased by around 25–30% in cultures from all donors (Fig. 6). The differences in thickness among the different donors observed at week 8 were still observed at week 11 after air-lift — the cultures from donors SA3 and SA4 presented a very thin epithelium at this time point.

One hallmark of small airway epithelia is the presence of club cells and a low number of goblet cells (Benam et al., 2016; Harvey et al., 2006). The same cultures that were used for hematoxylin, eosin, and Alcian blue staining were immunostained with anti-CC10 and anti-MUC5AC antibodies, markers for club and goblet cells, respectively. As expected, at week 8 after air-lift, the cultures showed an abundant presence of club cells (Fig. S2) but contained very few goblet cells (Fig. S3). At week 11, there was a notable decrease in club cell numbers in cultures from donors SA3 and SA4 (Fig. S2).

Next, we performed whole-mount staining with a β-tubulin 4 antibody to detect ciliated cells. As shown in Fig. 7, β-tubulin 4 staining revealed the presence of ciliated cells in all donors. However, the cultures from donors SA3 and SA4 exhibited a non-homogeneous morphology, with patchy distribution of ciliated cells; this was in contrast to the uniform distribution of ciliated cells in the cultures of the other donors, which was already observed at the histological level (Fig. 6). At week 11 after air-lift, the intensity of β-tubulin 4 staining had increased in all donor cultures relative to week 8, and this was confirmed by quantification of the total intensity of β-tubulin 4 spots (Fig. 8A). Analysis of the composition of variance showed that ~67% of the variance was caused by donor-to-donor variation, ~12% by the time factor, and the rest by residual variability (Fig. 8B).

3.3. Evaluation of tissue barrier function

The airway epithelia play a key role as a physical barrier against particles and toxicants. One measure of the integrity of the epithelial barrier is the product of its electrical (ohmic) resistance and epithelial surface area, known as TEER ($\Omega \cdot cm^2$). In this study, TEER was measured in bronchial cultures from 5 different donors longitudinally at weeks 5, 7, and 9 after air-lift. At week 5, the TEER values ranged from ~350 to 650 $\Omega \cdot cm^2$ (Fig. 9A). The cultures derived from donor BR5 displayed the highest TEER values, whereas those from donors BR1 and BR2 presented the lowest TEER values. With the exception of the cultures derived from donor BR3, the TEER values decreased over time, reaching values that were around 30% lower at week 9 than those at week 5.

We also evaluated TEER longitudinally in small airway cultures from 6 different donors at weeks 8, 9, 10, and 11 after air-lift. At week 8, the small airway cultures presented TEER values ranging from 550 to 950 $\Omega \cdot cm^2$, which were, on average, higher than in the values in the bronchial cultures (Fig. 9B). The cultures from donor SA5 presented, in general, the highest TEER values, whereas those from donor SA2 presented the lowest TEER. Similar to the trend observed in the bronchial cultures, a progressive decrease in TEER was seen in all donor cultures during the 4-week experimental period. The decline in TEER values was particularly severe in the cultures from donors SA3 and SA4 at the end of the experimental period

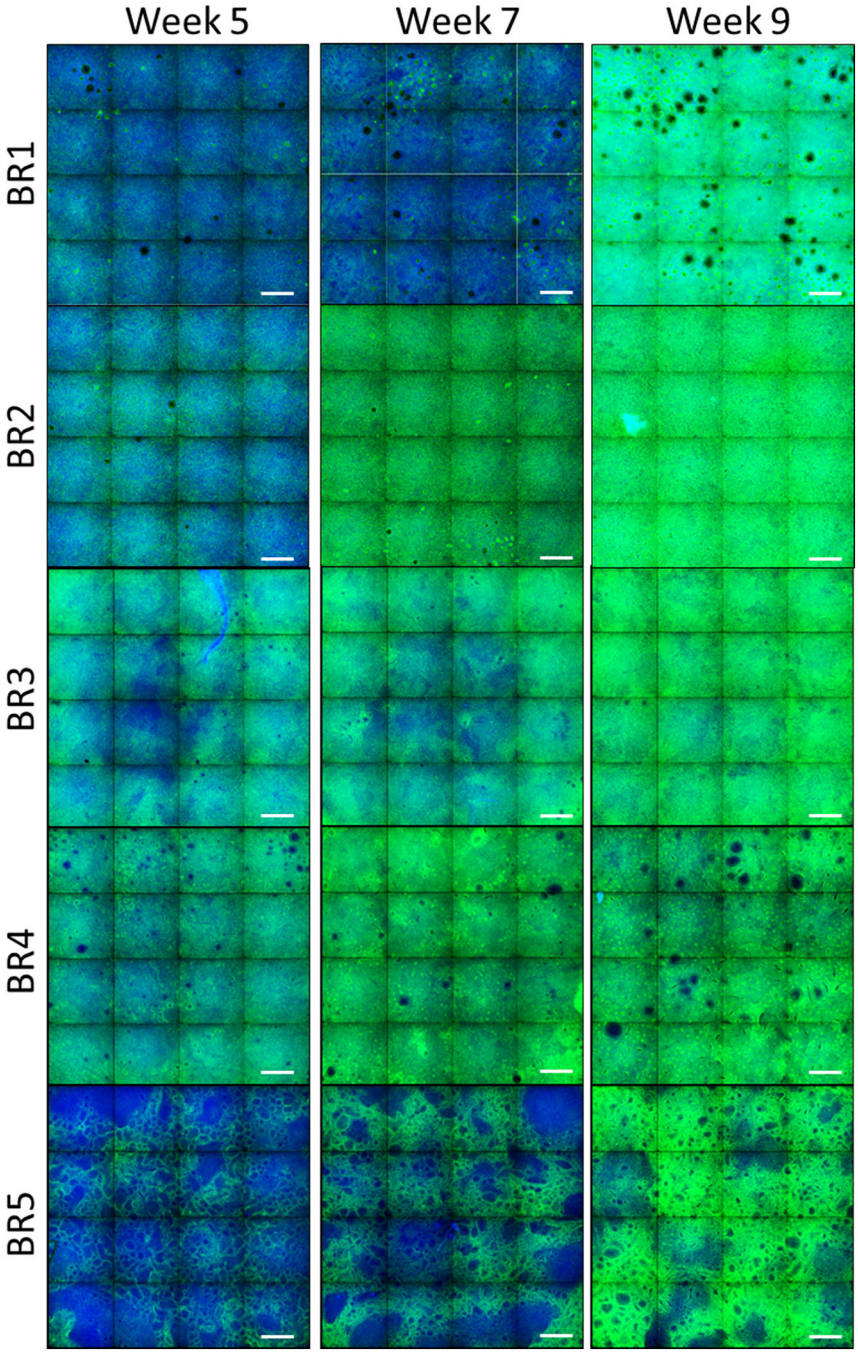

Fig. 2. β-Tubulin 4 immunofluorescence in bronchial cultures from different donors at weeks 5, 7, and 9 after air-lift. Representative images of bronchial cultures obtained from 5 different donors stained at different time points after air-lift with a β-tubulin 4 primary antibody conjugated to Alexa Fluor 647 (green) and Hoechst for nuclear staining (blue). Three (donors BR1 and BR2) or two (donors BR3–BR5) technical replicates were used for immunofluorescence analysis per time point. Each image is composed of 16 contiguous fields of view. Magnification: 10 ×. Scale bar: 400 μm. ×.

(week 11 after air-lift). The variance component analysis indicated that donor-to-donor variation was the principal source of variation (~94% in bronchial cultures; ~60% in small airway cultures). In the small airway cultures, almost a third of the variance was caused by residual variance (Fig. 9C and D).

3.4. Evaluation of cilia beating in bronchial and small airway cultures from different donors

Lung epithelia are covered in a layer of mucus, which can trap pathogens and particles present in the air and propel them to the back of the throat using small cilia, a phenomenon called mucociliary clearance (Powles-Glover, 2014). Cilia beating was measured weekly in the same inserts, first at the basal state and then after a 30-min stimulation with isoproterenol, a β-adrenergic agonist that increases CBF in airway epithelia (Agu et al., 1999).

The CBFs in untreated bronchial cultures were similar from week 5 to week 9 after air-lift (Fig. 10A). The cultures derived from donor BR1 presented the highest basal frequency (9.8–10.9 Hz) at week 5, while those derived from the 4 other donors had CBFs between 8 and 9 Hz. Isoproterenol treatment effectively stimulated the CBF in all donors. The responses were generally preserved across the assessment period, but the cultures from

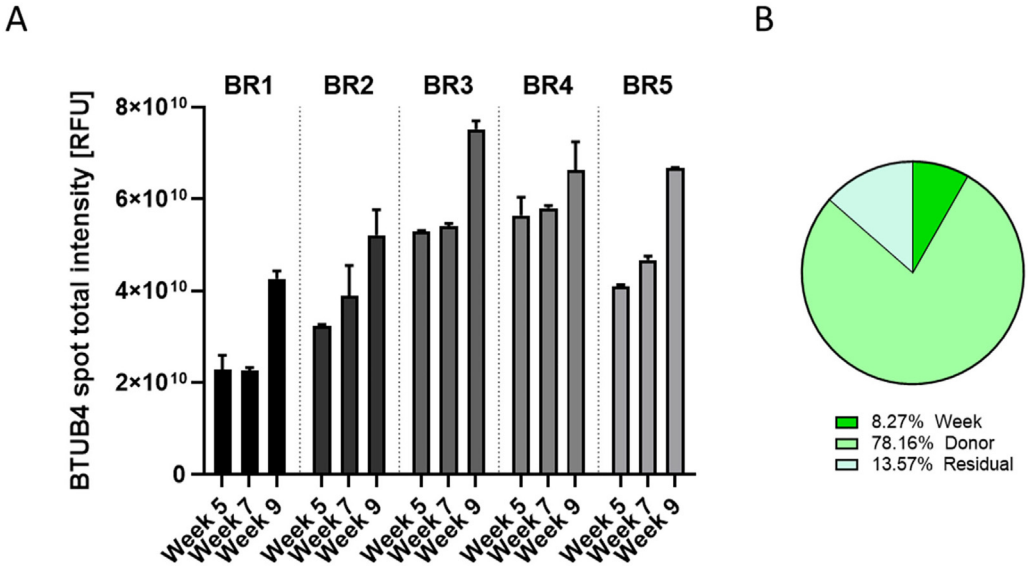

Fig. 3. Quantification of β-tubulin 4-positive cells in bronchial cultures from different donors at weeks 5, 7, and 9 after air-lift. (A) The intensity of all β-tubulin 4 spots visible in tissues stained with a β-tubulin 4 primary antibody was measured by using the CellInsight™ CX7 high-content screening platform. Data are presented as mean ± SEM for 3 (donors BR1 and BR2) or 2 (donors BR3–BR5) technical replicates per time point. (B) Variance components were estimated in bronchial cultures. The relative contributions of the donor and time (week), as well as those of residual factors, were estimated in the variance analysis. BTUB4 = β-tubulin 4; SEM = standard error of the mean.

donor BR1 were less responsive to isoproterenol treatment at weeks 7 and 9 after air-lift.

In untreated small airway cultures, CBF measurement also revealed some differences among the donors (Fig. 10B). In general, the cultures from donors SA3 and SA5 presented the highest CBF values (6.7–13.66 Hz), whereas those derived from donors SA1 and SA2 presented the lowest frequencies (9.84–5.17 Hz). We observed that the CBF increased from week 8 to week 11 after air-lift in all untreated donor cultures, except in donor SA2 cultures, in which they decreased over time. As expected, the CBF in cultures from all donors increased after the 30-min exposure to isoproterenol; however, the degree of induction varied among the donors, with cultures from donors SA1 and SA2 being the least responsive to isoproterenol stimulation.

When considering the 2 conditions separately (untreated and isoproterenol-treated cultures), approximately two-thirds of the total random variation was caused by the donor in both culture models (Fig. 10C and D).

3.5. CYP1A1/1B1 activity in bronchial and small airway cultures from different donors

CYP enzymes are responsible for metabolizing various substances, including carcinogens and other xenobiotics (Omiecinski et al., 2011). In this study, we evaluated the metabolic capacity of bronchial and small airway cultures obtained from different donors by longitudinally measuring the combined activity of CYP1A1 and CYP1B1, 2 of the main CYP isoforms present in the lungs (Castell et al., 2005). We evaluated CYP1A1 and CYP1B1 activity either in the basal condition (untreated cultures) or in cultures treated with TCDD, a compound that binds the aryl hydrocarbon receptor, which induces CYP1A1 and CYP1B1 expression and activity (Ramadoss et al., 2005).

The basal CYP1A1/1B1 activity was low in the bronchial cultures at all tested time points (Fig. 11A). However, after a 48-h treatment with TCDD, the CYP1A1/1B1 activity increased dramatically in all cultures. The magnitude of the TCDD response varied significantly among the donors: Compared with the basal enzyme activity, the TCDD treatment increased the activity of the enzyme by 60-fold in donor BR3 and by 330-fold in donor BR1 at week 5. Additionally, the induction of CYP1A1/1B1 enzyme activity in response to TCDD treatment increased over time in all donors: At week 9, the induced CYP1A1/1B1 enzyme activity was between 1.75- and 7.5-fold higher than that at week 5. In small airway cultures, the basal CYP1A1/1B1 activity was also low, but the combined CYP1A1/1B1 activity increased robustly in response to TCDD stimulation (Fig. 11B). Similar to what was observed in bronchial cultures, the magnitude of increase in CYP1A1/1B1 activity in response to TCDD treatment also varied substantially among the donors: Compared with the basal enzyme activity, the TCDD treatment increased the enzyme activity by 8.25-fold in donor SA4 and by 84-fold in donor SA1 at week 9. The extent of induction also increased over time in all donors: At week 11, the enzyme activity was between 2.4- and 10.7-fold higher than that at week 9.

When considering the 2 conditions separately (untreated and TCDD-treated cultures), approximately 20% and 27% of the total variance was caused by the donor in the bronchial and small airway cultures, respectively (Fig. 11C and D). For both culture types, approximately two-thirds of the total variance was caused by residual variance, which was more pronounced than that for CBF or TEER measurements. This non-defined source of variance could be attributed mainly to the variability of the technical replicates in the TCDD-exposed samples, a consequence of the high levels of fold induction and the technical complexity of a luminescence-based assay.

4. Discussion and conclusions

ALI lung cultures offer the possibility to test the toxicity of aerosols in a more physiological manner than submerged cultures. However, the use of primary cells for developing these tissues requires an understanding of the impact of the donor on tissue characteristics. In this study, we aimed to identify the sources of variability among different lung cultures derived from different donors. The outcome of the study might facilitate estimation of the donor number needed for a given experiment. We characterized 3D bronchial cultures developed in-house and commercially available 3D small airway epithelial cultures (SmallAir™, Epithelix) derived from different donors over several weeks in culture. The choice of using both commercially and non-commercially available cultures also allowed for overall assessment regardless of the technical protocols used for the development.

Overall, our study shows that 3D lung epithelial cultures prepared from different donors differed in their morphology; they presented variable epithelial thickness, relative cell composition, and presence/absence of cysts. In the non-commercial bronchial cultures, the difference in culture thickness among donors or at different time points was mainly due to a seemingly undifferentiated layer of cells present between the columnar and basal cells. Given their undifferentiated nature, we speculate that these

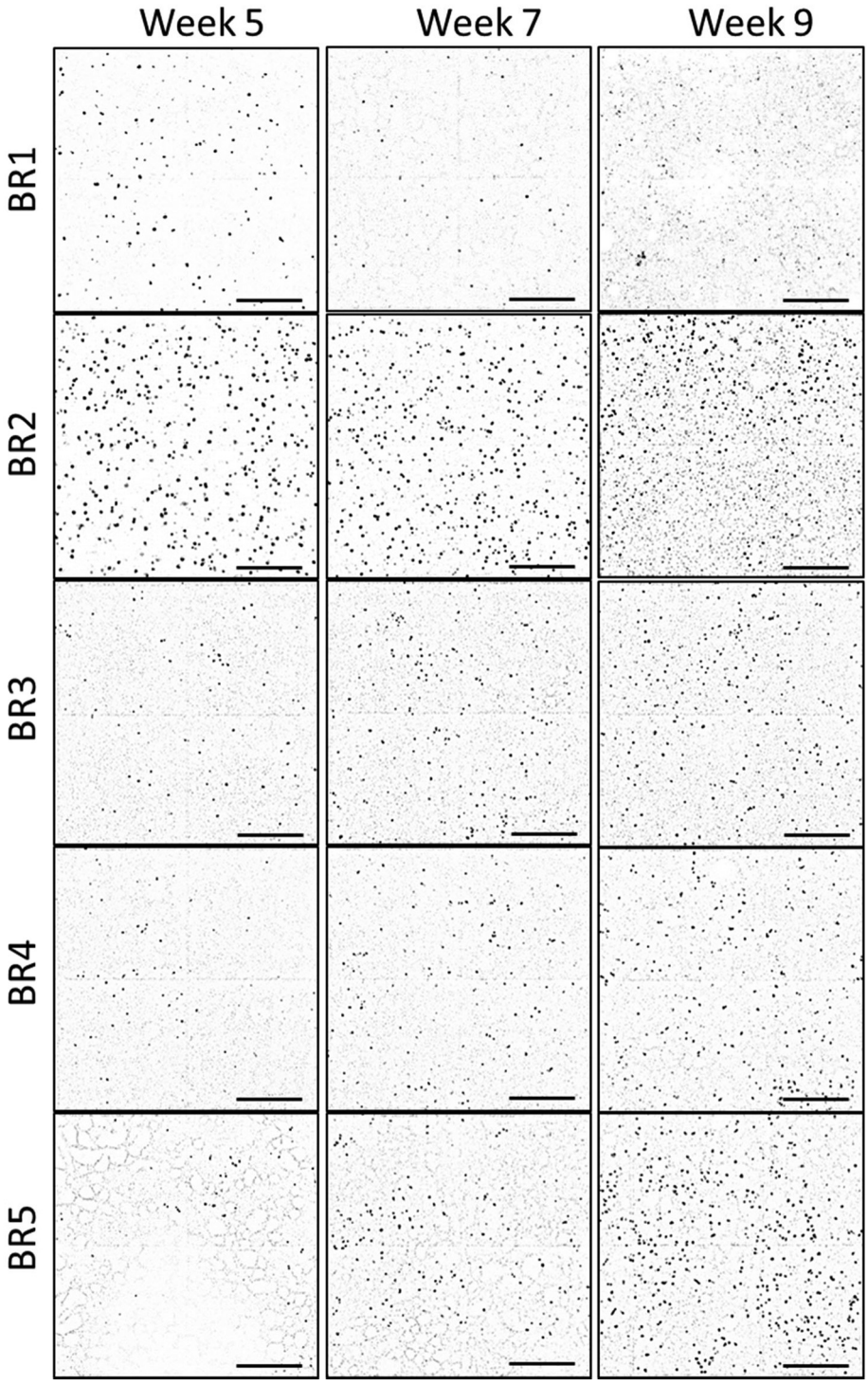

Fig. 4. Representative images of MU5AC (black dots)-stained bronchial tissues at weeks 5, 7, and 9 after air-lift. Representative images of bronchial cultures obtained from 5 different donors stained at different time points after air-lift with a MU5AC primary antibody conjugated to Alexa Fluor 555 (black spots). Three technical replicates were used for immunofluorescence analysis per time point. Each image is composed of 4 contiguous fields of view. Magnification: 10×. Scale bar: 400 μm.

cells were basal cells. The reason why this cell layer was more or less prominent in different donors is unknown. It is possible that some cultures were not completely mature or that basal cells from specific donors were more prone to proliferation (giving rise to basal cell hyperplasia) once the cells had differentiated.

The presence of cysts was another morphological feature specific to some donors. The cysts present in bronchial cultures were filled with mucus, as evidenced by the Alcian blue staining at the beginning of the experimental period, but they were not stained at later time points. The mucus was not likely composed of MU5AC, because we would have otherwise detected these large structures with the whole-insert immunostaining approach. In contrast, the cysts observed in the small airway cultures obtained from donor SA2 remained full of polysaccharides during the experimental period. The reason for the formation of these cysts remains unknown and has, to our knowledge, not been described in the literature. We hypothesize that they might be caused by abnormally low intracellular and extracellular calcium stores (Bou-Hanna et al., 1994) or low bicarbonate concentrations (Gorrieri et al., 2016; Liu et al., 2015) or by defective

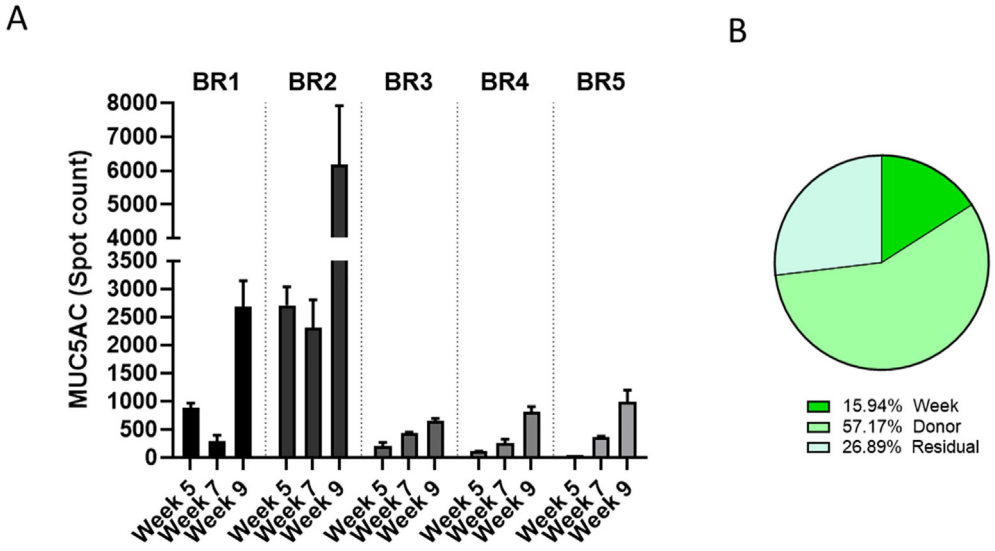

Fig. 5. Quantification of MUC5AC-positive spots in bronchial cultures from different donors at weeks 5, 7, and 9 after air-lift. (A) The number of mucin 5 AC-positive spots visible in tissues stained with a MUC5AC primary antibody was measured by using the CellInsight™ CX7 high-content screening platform. Data are presented as mean ± SEM for 3 (donors BR1 and BR2) or 2 technical replicates (donors BR3–BR5) per time point. (B) Variance components were estimated in bronchial cultures. The relative contributions of the donor and time (week), as well as those of residual factors, were estimated in the variance analysis. MUC5AC = mucin 5 AC; SEM = standard error of the mean.

ATP signaling (Adler et al., 2013) causing the goblet cells to release their mucus not at the surface of the tissue but rather in the middle of the epithelium, leading to these inner pockets (cysts). The number of cysts per bronchial tissue varied from batch to batch, but we observed a strong relationship between the donor and the abundance of visible cysts. This suggests that the presence of cysts was not an experimental artifact of this particular set of experiments but a feature of the cultures obtained from specific donors. Although we show that in our study, culture functionality (i.e., CBF, TEER, and CYP1A11B1 activity) was not severely impacted by the presence of these cysts, we have observed that cultures with cysts tend to evolve rapidly at the morphological level and present a higher degree of insert-to-insert morphological variability. In addition, the molecular effects of the cysts and their effect on epithelial permeability remain unknown and should be better characterized to determine whether these cultures can be used for certain experimental purposes. Notably, we observed that the small airway cultures presented less morphological diversity

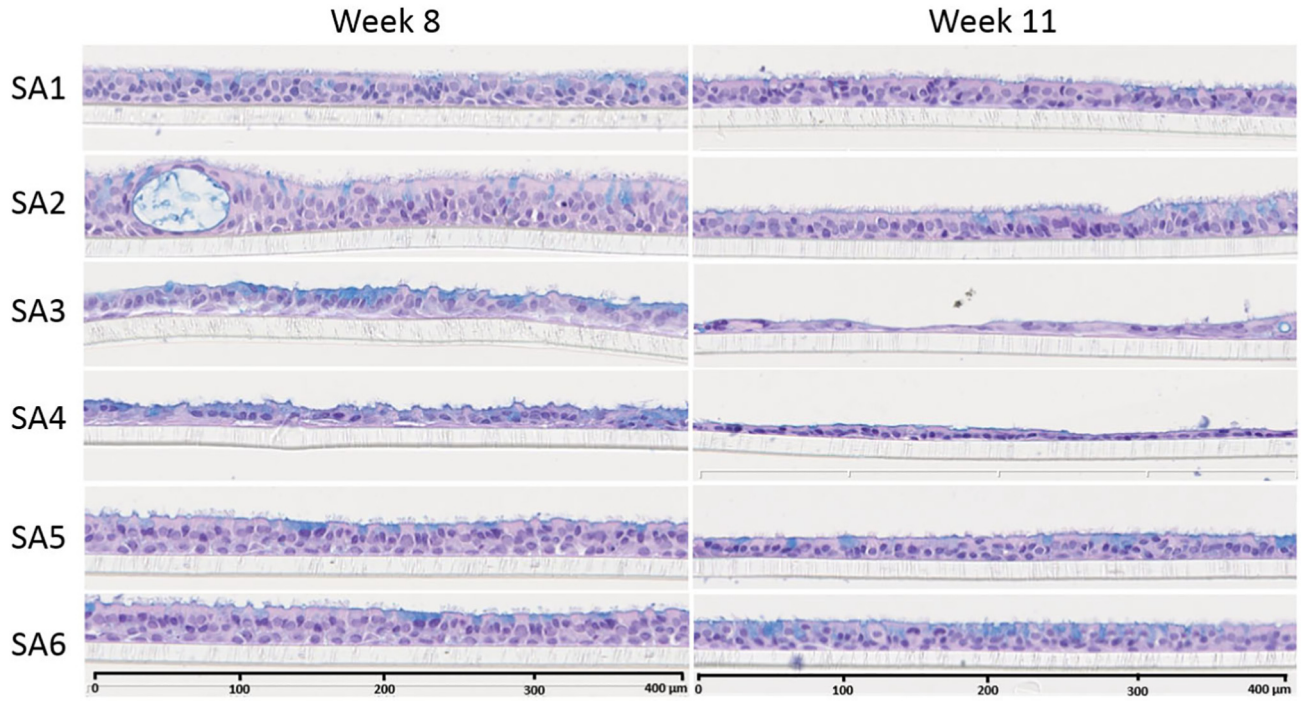

Fig. 6. Representative histological sections of small airway cultures from different donors at weeks 8 and 11 after air-lift. Representative images of small airway culture sections stained with hematoxylin, eosin, and Alcian blue from cultures obtained from 6 different donors collected at week 8 (left) and week 11 (right) after the air-lift. Three technical replicates were used for histological analysis per time point. Magnification: 20×.

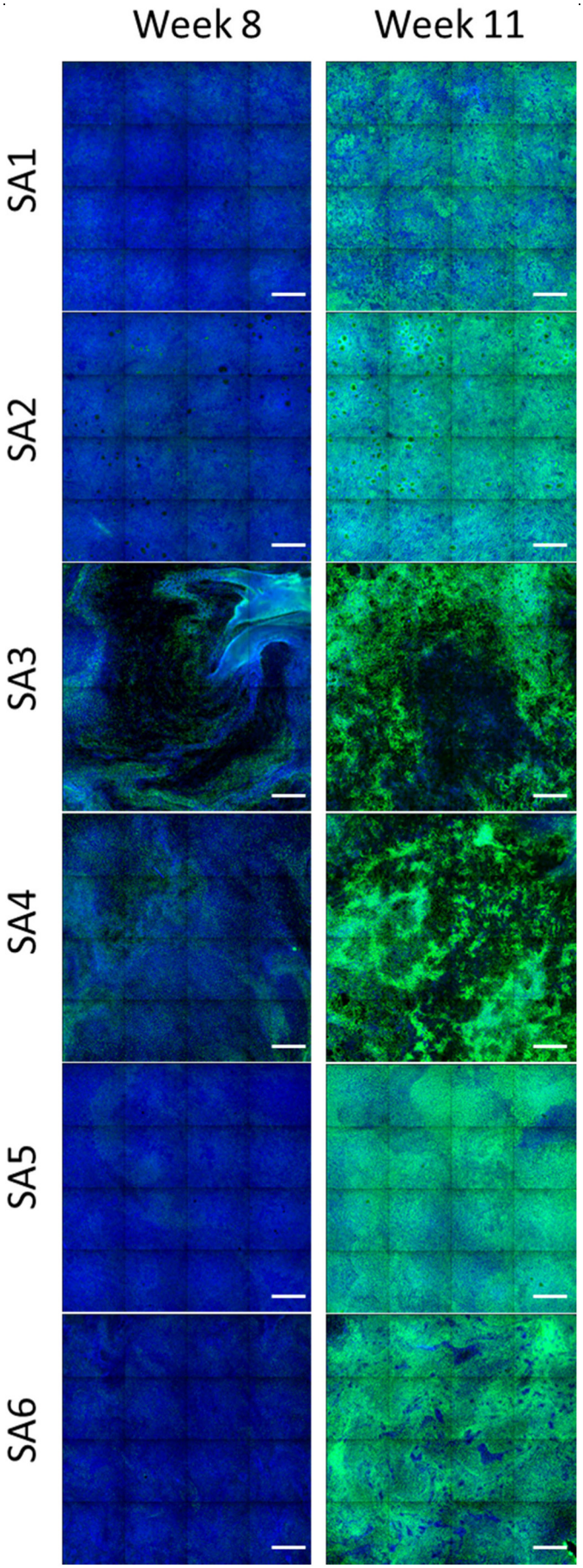

compared with the bronchial cultures prepared in-house. Because the former were commercially available (SmallAir™, Epithelix), it is likely that quality checks (often based on TEER measurement and morphological analysis) had already been performed to preselect donors whose cells formed cultures with optimal morphology and discard those whose cells yielded suboptimal cultures.

In addition to the differences observed in culture morphology among the donors, the functionality readouts (TEER and CBF) also showed some differences depending on the donor. For instance, TEER values varied among the donors in both culture types. Huang and colleagues previously compared SmallAir™ cultures prepared by using basal cells from 5 different donors and observed a similar variability in TEER and CBF among the donors (Huang et al., 2017). In contrast, Tosoni and colleagues described a much greater variability in TEER values in primary nasal cultures obtained from 18 different healthy donors. In their study, the TEER values showed non-normal distribution, with a significant number of donors at both extremes of the distribution (Tosoni et al., 2016). In our study, we were unable to determine the association between TEER and the morphological aspect of the cultures. In fact, cultures that were thin or had cysts did not display lower TEER than those that were thicker or did not have cysts. Notably, we observed a progressive decrease in TEER values over time after air-lift in both culture types and in all donors tested. While this decrease could be due to the aging of the cultures, we strongly believe that the decrease in TEER over time was mainly caused by the repeated (longitudinal) measurement of TEER (i.e., the cultures were frequently subjected to fluid submersion, required for TEER measurement). Indeed, we observed that the bronchial cultures used for TEER measurement presented lower TEER values than the untreated cultures (data not shown). Exposure of lung epithelial cells to cell culture medium is likely to affect the apical surface liquid tonicity, which has been demonstrated to rapidly increase proteolytic ion transport and, later on, the translocation of aquaporins at the plasma membrane (Schmidt et al., 2017). Expression of these channels at the plasma membrane could decrease the electrical resistance resulting from the phospholipid barrier and explain the TEER decrease measured over time in longitudinally exposed cultures. Thus, we recommend against repeated measurement of TEER in the same 3D lung epithelial cultures.

Our study showed that isoproterenol treatment resulted in a remarkably preserved CBF stimulation across donors and tissue types. Similarly, TCCD treatment robustly induced CYP1A1/1B1 activity in all cultures, independently of the culture type and donor, although the magnitude of the induction varied. Because TCDD has a long half-life (Pirkle et al., 1989), it is likely that the progressive increase in CYP1A1/1B1 induction was caused by accumulation of TCDD in the cultures. Interestingly, some donor cultures showed a more robust induction of CYP1A1/1B1 activity over time, which was not correlated with the fold induction observed at the beginning of the experimental period. We speculated that the differences in CYP1A1/1B1 activity among the donors could be due either to polymorphisms in CYP1A1/1B1 (Landi et al., 2005) or the aryl hydrocarbon receptor (AhR) (Kovalova et al., 2016) or to the levels of CYP1A1/1B1 gene expression (Boei et al., 2017), which, in turn, could have different causes (e.g., genetic variation and exposure history). Our observations are aligned with those of previous studies using ALI lung models, showing preserved responses to certain stimuli across donors despite variations in intensity. For instance, the secretion profile of proinflammatory mediators (Banerjee et al., 2017) and the changes in gene expression in response to cigarette smoke exposure (Haswell et al., 2017; Iskandar et al., 2017b) as well as the inflammatory response following ozone exposure (Bowers et al., 2018) followed similar patterns across

Fig. 7. β-Tubulin 4 immunofluorescence in small airway cultures from different donors at weeks 8 and 11 after air-lift. Representative images of small airway cultures from different donors stained with a β-tubulin 4 primary antibody coupled to Alexa 647 fluorescent dye (green) and Hoechst dye for nuclear staining (blue) at weeks 8 and 11 after air-lift. Each image is composed of 16 contiguous fields of view. Magnification: 10×. Scale bar: 400 μm.×.

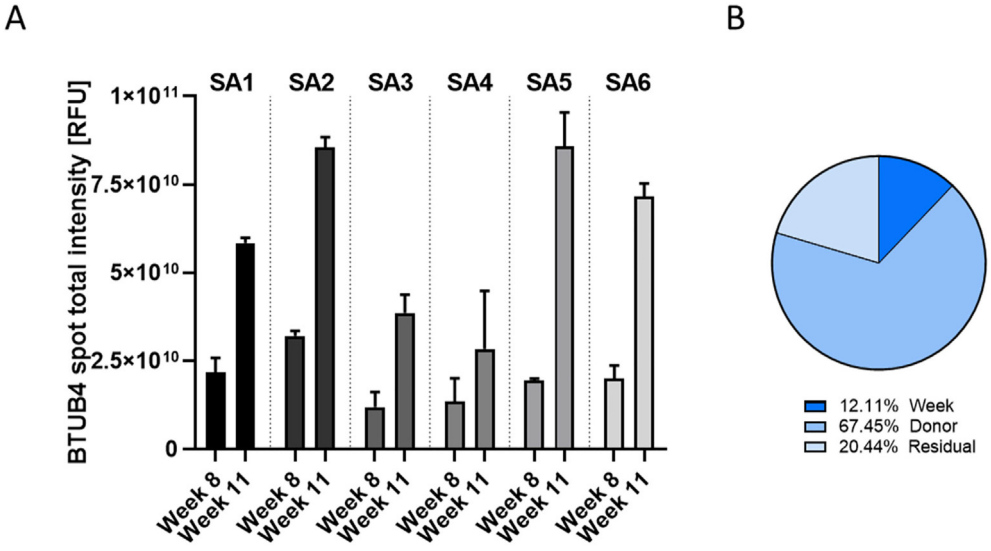

Fig. 8. Quantification of β-tubulin 4-positive cells in small airway cultures from different donors at weeks 8 and 11 after air-lift. (A) The intensity of all β-tubulin 4 spots visible in tissues stained with a β-tubulin 4 primary antibody was measured by using the CellInsight™ CX7 high-content screening platform. Data are presented as mean ± SEM for 2 technical replicates per donor for each time point. (B) Variance components were estimated in small airway cultures. The relative contributions of the donor and time (week), as well as those of residual factors, were estimated in the variance analysis. BTUB4 = β-tubulin 4; SEM = standard error of the mean.

cultures from different donors, although they varied in magnitude. In contrast, the inflammatory response of airway cultures to influenza virus infection seems to be more impacted by the donor of the cultures (Ilyushina et al., 2019), which suggests that interdonor variability should be specifically addressed for each endpoint and experimental condition tested.

Because of the low number of donors used in the present study, we could not establish any association between the donor characteristics and culture features. This should be addressed by using a larger number of donors to independently study the potential impact of a given fixed parameter (age, sex, ethnicity, smoking status, enzyme polymorphism, medical history, etc.) on a specific variable of interest. Notably, the origin of the differences observed in culture morphology and the magnitude of response of the cultures to different stimuli (in our case, isoproterenol and TCDD) could also be due to the preparation of the cultures (isolation of basal cells, cell passage, culture handling, batch-effects due to freeze/thaw cycles, etc.). Future studies could compare 3D cultures prepared from basal cells from the same donor but from different repetitions of the cell isolation procedure. This could help disentangle donor-specific effects from the potential effects related to the preparation of the cultures. Nevertheless, even if the latter hypothesis was discarded, the question about the specific sources of interdonor variability would remain.

While the number of donors should, in principle, be as large as possible in order to be representative of the population, the number of donors used in a study will be limited by the availability of cells or cultures from multiple donors as well as the cost and/or difficulties in handling large numbers of cultures. As it is often not possible to use cultures derived from a large number of donors, our results suggest that the number of donors needed will depend on the purpose of the study. For example, because the responses to TCDD and isoproterenol were preserved among the donors, studies focusing on CYP1A1/1B1 induction or the response of cultures to CBF-stimulating agents probably do not require multiple donors, whereas studies focusing on tissue morphology might need to include tissues from multiple donors. Our study shows that donor from whom a culture is derived can have a major effect on the data generated, if the study is based on morphological criteria, as might be the case in studies on comparison of cultures from healthy and diseased donors. Results from studies of this type or those using culture morphology as an endpoint should be carefully interpreted when the donor's lung cells give rise to thick cultures or cultures with cysts. Indeed, their rapidly evolving morphology and greater morphological variability from culture to culture can result in erroneous conclusions. To better understand the mechanisms leading to the formation of these specific features in some cultures, we encourage future studies on comparison of various donors to also include transcriptomic and proteomic analyses. An alternative approach to using cultures from several donors could be the pooling of primary cells of multiple donors into a single 3D culture aiming to generate lung tissues that resemble the average response of a population (Balogh Sivars et al., 2018). Such models with pooled donors would be sufficient for investigating the potential toxicity of compounds, although they will likely be less suitable for studying gene expression, considering the unique genetic makeup of each individual donor.

Finally, lung primary cultures grown at the ALI currently represent one of the most advanced lung in vitro models for studying the toxicity of aerosols or inhaled drugs. Collaboration between public organizations, academia, and the industry would boost the further development of these types of cultures, along with new analytical tools, which could represent an interesting alternative to the use of animal models in respiratory toxicology. Overall, our results indicated that, regardless of their diverse morphology, lung cultures obtained from different donors show a similar response to stimuli in terms of functionality and metabolic capacity. To evaluate the utility of these cultures in drug testing, including the necessity for multi-donor study designs, a similar study should be conducted in the future with defined treatment conditions and endpoints.

Funding

Philip Morris International is the sole source of funding and sponsor of this research.

Declaration of competing interest

The authors declare the following financial interests/personal relationships which may be considered as potential competing interests: All authors are employees of Philip Morris International.

Acknowledgments

We would like to thank Nicholas Karoglou and Sindhoora Bhargavi Gopala Reddy for critical review of the manuscript; Stephanie Boue and Fabian Moine for adding the data of the present study on the INTERVALS platform.

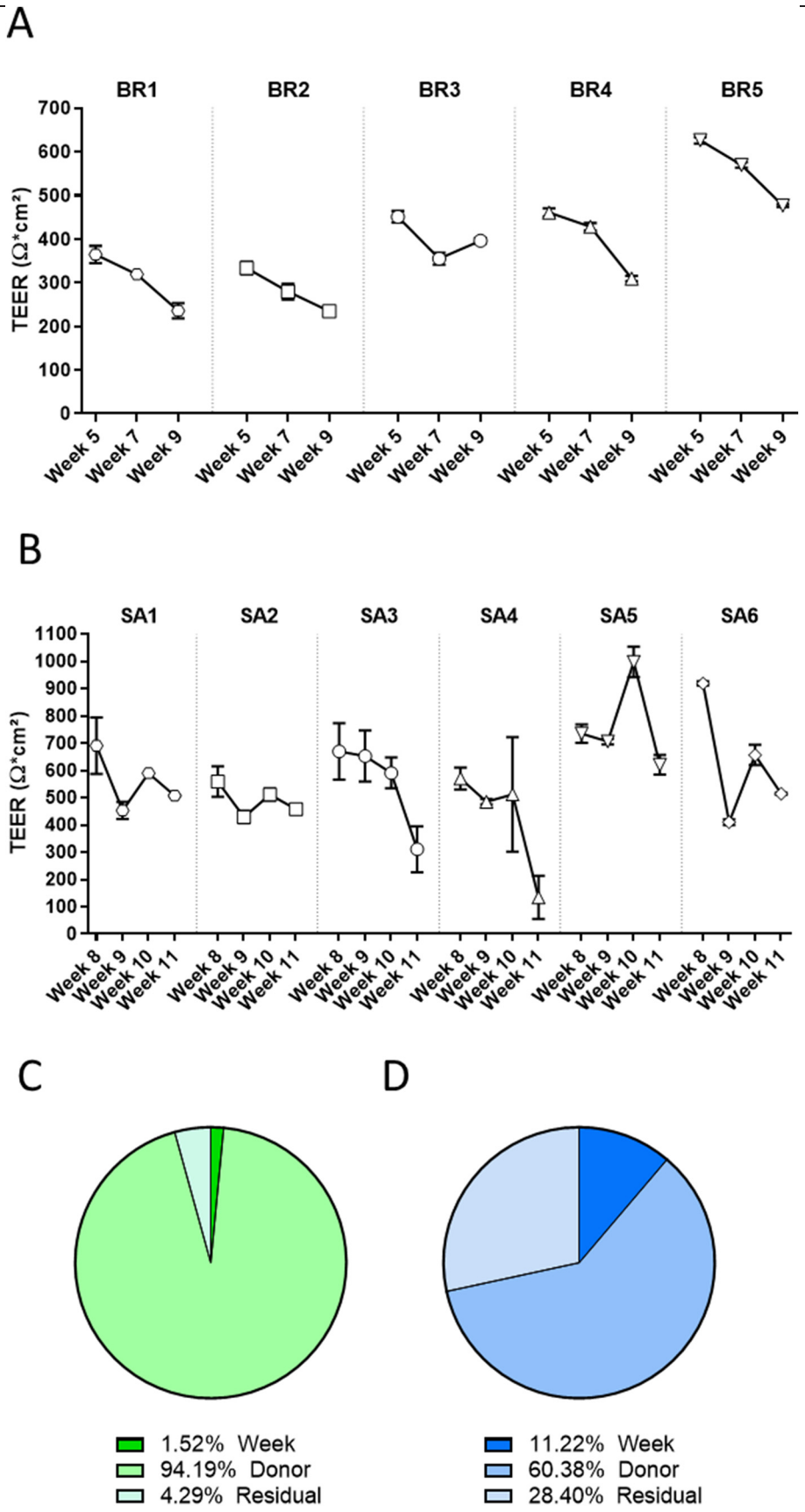

Fig. 9. Longitudinal TEER measurement in bronchial and small airway cultures. TEER was measured longitudinally at weeks 5, 7, and 9 after air-lift in the same subset of bronchial cultures (A) and at weeks 8, 9, 10, and 11 after air-lift in the same subset of small airway cultures (B) obtained from different donors. Data are presented as mean ± SEM for $n = 4$ (bronchial) and $n = 3$ (small airway) independent cultures. Variance components were estimated in bronchial (C) and small airway (D) cultures. The relative contributions of the donor and time (week), as well as those of residual factors, were estimated in the variance analysis. SEM = standard error of the mean.

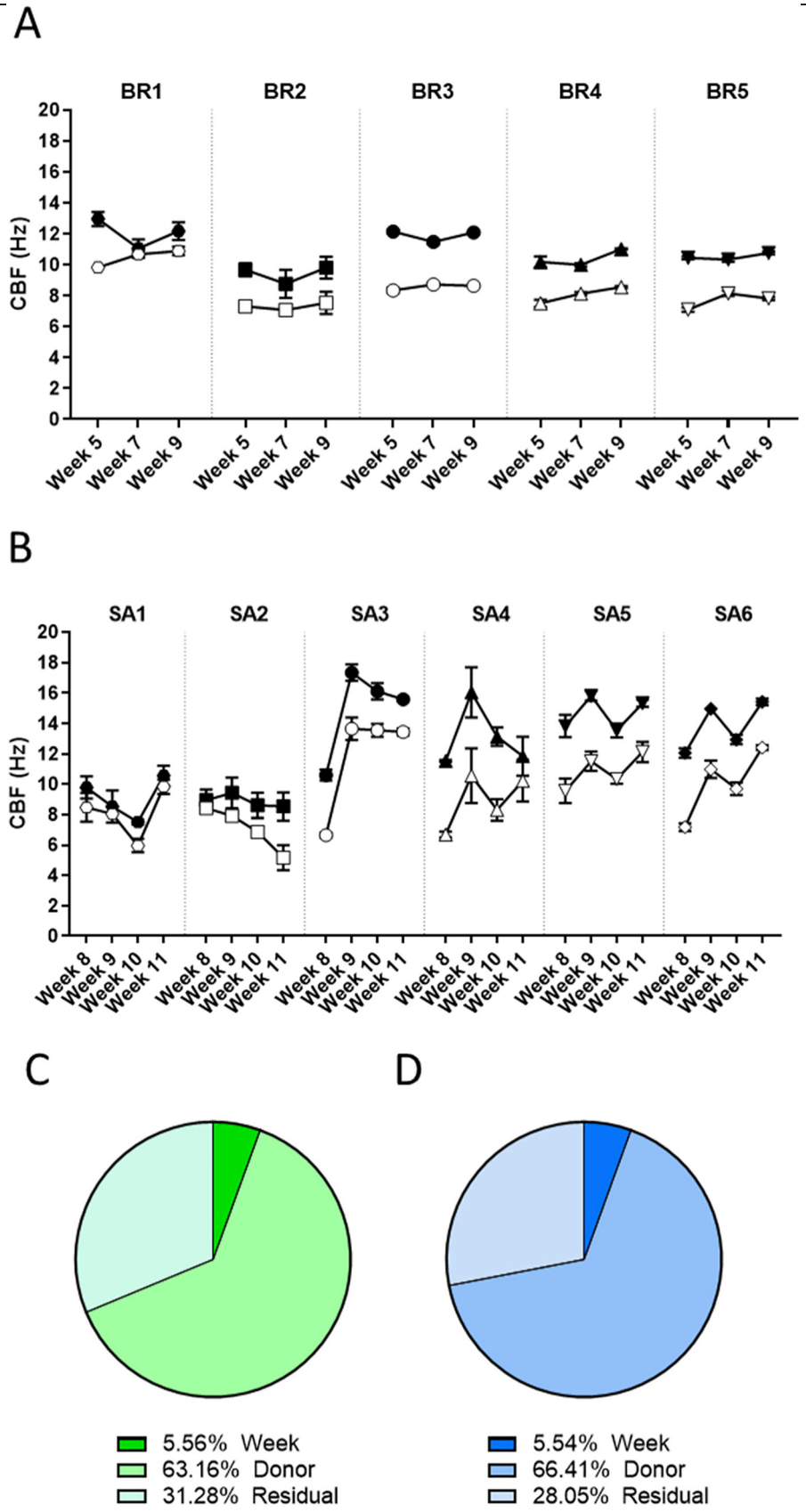

Fig. 10. CBF in bronchial and small airway cultures. CBF was measured longitudinally at weeks 5, 7, and 9 after air-lift in the same subset of bronchial cultures (A) and at weeks 8, 9, 10, and 11 after air-lift in the same subset of small airway cultures (B) from different donors at the basal level (untreated cultures; open symbols) and after a 30-min stimulation with isoproterenol (filled symbols). Data are presented as mean ± SEM for $n = 4$ (bronchial) and $n = 3$ (small airway) independent cultures. Variance components were estimated in bronchial (C) and small airway (D) cultures. The relative contributions of the donor and time (week), as well as those of residual factors, were estimated in the variance analysis. CBF = cilia beating frequency; SEM = standard error of the mean.

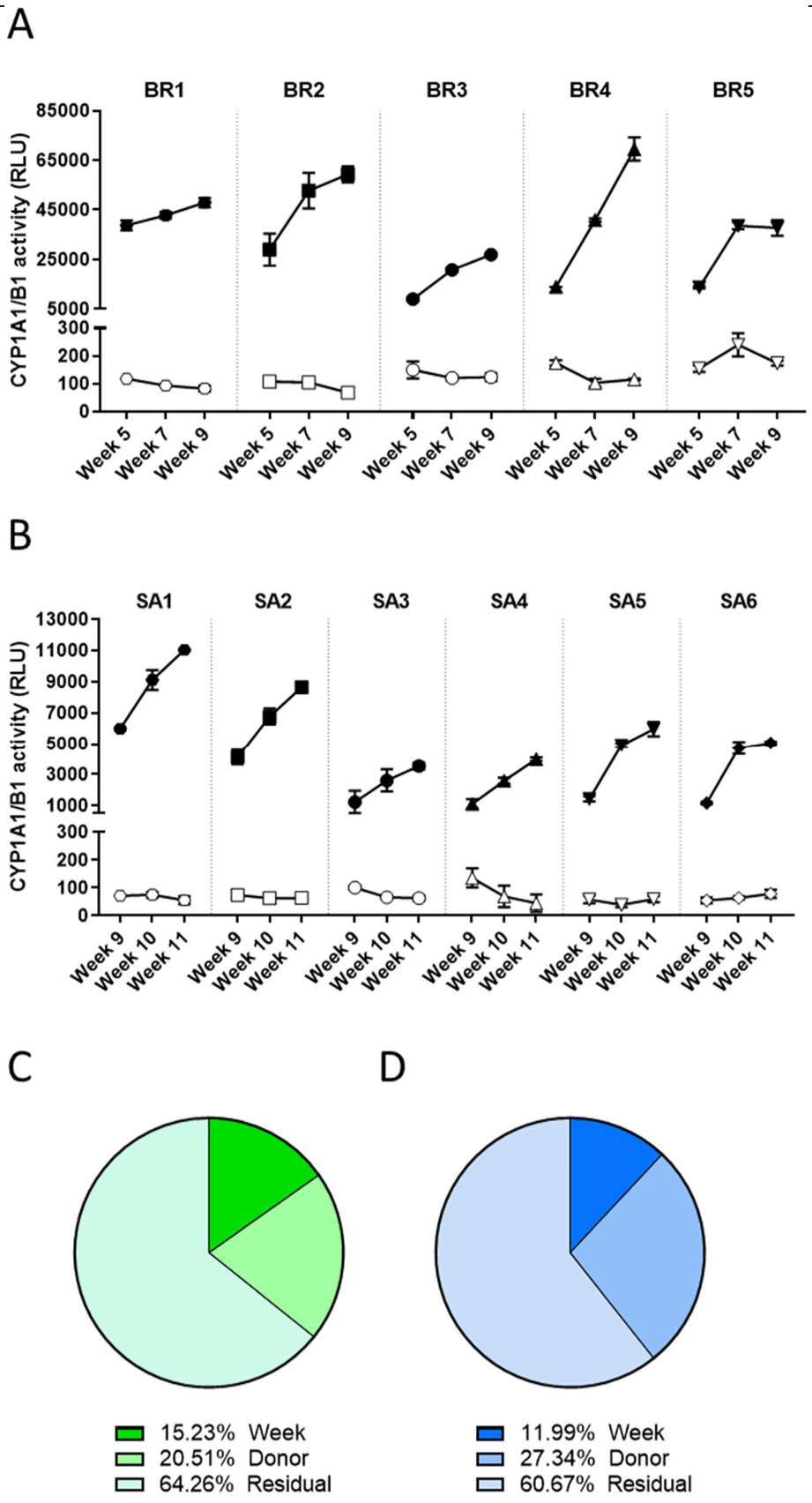

Fig. 11. CYP1A1/1B1 activity in bronchial and small airway cultures. CYP1A1/1B1 activity was measured longitudinally at weeks 5, 7, and 9 after air-lift in the same subset of bronchial cultures (A) and at weeks 8, 9, 10, and 11 after air-lift in the same subset of small airway cultures (B) from different donors at the basal level (open symbols) and after a 48-h stimulation with TCDD (filled symbols). Data are presented as mean ± SEM for 3 independent cultures per donor. Variance components were estimated in bronchial (C) and small airway (D) cultures. The relative contribution of donor and time (week), as well as of residual factors were estimated in the variance analysis. CYP = cytochrome P450; RLU = relative light unit; TCDD = 2,3,7,8-tetrachlorodibenzodioxin; SEM = standard error of the mean.

Appendix A. Supplementary data

Supplementary data to this article can be found online at https://doi.org/10.1016/j.crtox.2020.08.002.

References

Adler, K.B., Tuvim, M.J., Dickey, B.F., 2013. Regulated mucin secretion from airway epithelial cells. Front. Endocrinol. 4. https://doi.org/10.3389/fendo.2013.00129.

Agu, R.U., Jorissen, M., Willems, T., Van den Mooter, G., Kinget, R., Augustijns, P., 1999. Effects of pharmaceutical compounds on ciliary beating in human nasal epithelial cells: a comparative study of cell culture models. Pharm. Res. 16, 1380–1385.

Balogh Sivars, K., Sivars, U., Hornberg, E., Zhang, H., Brändén, L., Bonfante, R., et al., 2018. A 3D human airway model enables prediction of respiratory toxicity of inhaled drugs in vitro. Toxicol. Sci. 162, 301–308. https://doi.org/10.1093/toxsci/kfx255.

Banerjee, A., Haswell, L.E., Baxter, A., Parmar, A., Azzopardi, D., Corke, S., et al., 2017. Differential gene expression using RNA sequencing profiling in a reconstituted airway epithelium exposed to conventional cigarette smoke or electronic cigarette aerosols. Applied In Vitro Toxicology 3, 84–98. https://doi.org/10.1089/aivt.2016.0024.

Baxter, A., Thain, S., Banerjee, A., Haswell, L., Parmar, A., Phillips, G., et al., 2015. Targeted omics analyses, and metabolic enzyme activity assays demonstrate maintenance of key mucociliary characteristics in long term cultures of reconstituted human airway epithelia. Toxicol. in Vitro 29, 864–875. https://doi.org/10.1016/j.tiv.2015.03.004.

Benam, K.H., Villenave, R., Lucchesi, C., Varone, A., Hubeau, C., Lee, H.-H., et al., 2016. Small airway-on-a-chip enables analysis of human lung inflammation and drug responses in vitro. Nat. Methods 13, 151–157. https://doi.org/10.1038/nmeth.3697.

Boei, J.J.W.A., Vermeulen, S., Klein, B., Hiemstra, P.S., Verhoosel, R.M., Jennen, D.G.J., et al., 2017. Xenobiotic metabolism in differentiated human bronchial epithelial cells. Arch. Toxicol. 91, 2093–2105. https://doi.org/10.1007/s00204-016-1868-7.

Bou-Hanna, C., Berthon, B., Combettes, L., Claret, M., Laboisse, C.L., 1994. Role of calcium in carbachol- and neurotensin-induced mucin exocytosis in a human colonic goblet cell line and cross-talk with the cyclic AMP pathway. Biochem. J. 299 (Pt 2), 579–585.

Bovard, D., Sandoz, A., Luettich, K., Frentzel, S., Iskandar, A., Marescotti, D., et al., 2018. A lung/liver-on-a-chip platform for acute and chronic toxicity studies. Lab Chip 18, 3814–3829. https://doi.org/10.1039/C8LC01029C.

Bowers, E.C., McCullough, S.D., Morgan, D.S., Dailey, L.A., Diaz-Sanchez, D., 2018. ERK1/2 and p38 regulate inter-individual variability in ozone-mediated IL-8 gene expression in primary human bronchial epithelial cells. Sci. Rep. 8, 9398. https://doi.org/10.1038/s41598-018-27662-0.

Braun, L., Wolfgang, M., Dickersin, K., 2013. Defining race/ethnicity and explaining difference in research studies on lung function. Eur. Respir. J. 41, 1362–1370. https://doi.org/10.1183/09031936.00091612.

Carey, M.A., Card, J.W., Voltz, J.W., Arbes, S.J., Germolec, D.R., Korach, K.S., et al., 2007. It's all about sex: gender, lung development and lung disease. Trends in Endocrinology & Metabolism 18, 308–313. https://doi.org/10.1016/j.tem.2007.08.003.

Castell, J.V., Teresa Donato, M., Gómez-Lechón, M.J., 2005. Metabolism and bioactivation of toxicants in the lung. The in vitro cellular approach. Exp. Toxicol. Pathol. 57, 189–204. https://doi.org/10.1016/j.etp.2005.05.008.

Czekala, L., Simms, L., Stevenson, M., Tschierske, N., Maione, A.G., Walele, T., 2019. Toxicological comparison of cigarette smoke and e-cigarette aerosol using a 3D in vitro human respiratory model. Regul. Toxicol. Pharmacol. 103, 314–324. https://doi.org/10.1016/j.yrtph.2019.01.036.

Ghio, A.J., Dailey, L.A., Soukup, J.M., Stonehuerner, J., Richards, J.H., Devlin, R.B., 2013. Growth of human bronchial epithelial cells at an air-liquid interface alters the response to particle exposure. Part. Fibre Toxicol. 10, 25. https://doi.org/10.1186/1743-8977-10-25.

Gorrieri, G., Scudieri, P., Caci, E., Schiavon, M., Tomati, V., Sirci, F., et al., 2016. Goblet cell hyperplasia requires high bicarbonate transport to support mucin release. Sci. Rep. 6. https://doi.org/10.1038/srep36016.

Gray, T.E., Guzman, K., Davis, C.W., Abdullah, L.H., Nettesheim, P., 1996. Mucociliary differentiation of serially passaged normal human tracheobronchial epithelial cells. Am. J. Respir. Cell Mol. Biol. 14, 104–112. https://doi.org/10.1165/ajrcmb.14.1.8534481.

Hackett, T.-L., Singhera, G.K., Shaheen, F., Hayden, P., Jackson, G.R., Hegele, R.G., et al., 2011. Intrinsic phenotypic differences of asthmatic epithelium and its inflammatory responses to respiratory syncytial virus and air pollution. Am. J. Respir. Cell Mol. Biol. 45, 1090–1100. https://doi.org/10.1165/rcmb.2011-0031OC.

Harvey, B.-G., Heguy, A., Leopold, P.L., Carolan, B.J., Ferris, B., Crystal, R.G., 2006. Modification of gene expression of the small airway epithelium in response to cigarette smoking. J. Mol. Med. 85, 39–53. https://doi.org/10.1007/s00109-006-0103-z.

Hastedt, J.E., Bäckman, P., Clark, A.R., Doub, W., Hickey, A., Hochhaus, G., et al., 2016. Scope and relevance of a pulmonary biopharmaceutical classification system AAPS/FDA/USP Workshop March 16-17th, 2015 in Baltimore, MD. AAPS Open 2, 1. https://doi.org/10.1186/s41120-015-0002-x.

Haswell, L.E., Baxter, A., Banerjee, A., Verrastro, I., Mushonganono, J., Adamson, J., et al., 2017. Reduced biological effect of e-cigarette aerosol compared to cigarette smoke evaluated in vitro using normalized nicotine dose and RNA-seq-based toxicogenomics. Sci. Rep. 7, 888. https://doi.org/10.1038/s41598-017-00852-y.

Huang, S., Boda, B., Vernaz, J., Ferreira, E., Wiszniewski, L., Constant, S., 2017. Establishment and characterization of an in vitro human small airway model (SmallAir™). Eur. J. Pharm. Biopharm. 118, 68–72. https://doi.org/10.1016/j.ejpb.2016.12.006.

Ilyushina, N.A., Dickensheets, H., Donnelly, R.P., 2019. A comparison of interferon gene expression induced by influenza A virus infection of human airway epithelial cells from two different donors. Virus Res. 264, 1–7. https://doi.org/10.1016/j.virusres.2019.02.002.

Iskandar, A.R., Martinez, Y., Martin, F., Schlage, W.K., Leroy, P., Sewer, A., et al., 2017a. Comparative effects of a candidate modified-risk tobacco product aerosol and cigarette smoke on human organotypic small airway cultures: a systems toxicology approach. Toxicol. Res. 6, 930–946. https://doi.org/10.1039/C7TX00152E.

Iskandar, A.R., Mathis, C., Schlage, W.K., Frentzel, S., Leroy, P., Xiang, Y., et al., 2017b. A systems toxicology approach for comparative assessment: biological impact of an aerosol from a candidate modified-risk tobacco product and cigarette smoke on human organotypic bronchial epithelial cultures. Toxicol. in Vitro 39, 29–51. https://doi.org/10.1016/j.tiv.2016.11.009.

Iskandar, A.R., Martin, F., Leroy, P., Schlage, W.K., Mathis, C., Titz, B., et al., 2018. Comparative biological impacts of an aerosol from carbon-heated tobacco and smoke from cigarettes on human respiratory epithelial cultures: a systems toxicology assessment. Food Chem. Toxicol. 115, 109–126. https://doi.org/10.1016/j.fct.2018.02.063.

Ji, J., Hedelin, A., Malmlöf, M., Kessler, V., Seisenbaeva, G., Gerde, P., et al., 2017. Development of combining of human bronchial mucosa models with XposeALI® for exposure of air pollution nanoparticles. PLoS One 12, e0170428. https://doi.org/10.1371/journal.pone.0170428.

Karp, P.H., Moninger TO, Weber, S.P., Nesselhauf, T.S., Launspach, J.L., Zabner, J., et al., 2002. An In Vitro Model of Differentiated Human Airway Epithelia: Methods for Establishing Primary Cultures. Epithelial Cell Culture Protocols vol. 188. Humana Press, New Jersey, pp. 115–137. https://doi.org/10.1385/1-59259-185-X:115.

Kovalova, N., Manzan, M., Crawford, R., Kaminski, N., 2016. Role of aryl hydrocarbon receptor polymorphisms on TCDD-mediated CYP1B1 induction and IgM suppression by human B cells. Toxicol. Appl. Pharmacol. 309, 15–23. https://doi.org/10.1016/j.taap.2016.08.011.

Landi, M.T., Bergen, A.W., Baccarelli, A., Patterson, D.G., Grassman, J., Ter-Minassian, M., et al., 2005. CYP1A1 and CYP1B1 genotypes, haplotypes, and TCDD-induced gene expression in subjects from Seveso, Italy. Toxicology 207, 191–202. https://doi.org/10.1016/j.tox.2004.08.021.

Liu, J., Walker, N.M., Ootani, A., Strubberg, A.M., Clarke, L.L., 2015. Defective goblet cell exocytosis contributes to murine cystic fibrosis–associated intestinal disease. J. Clin. Investig. 125, 1056–1068. https://doi.org/10.1172/JCI73193.

Marescotti, D., Bovard, D., Morelli, M., Sandoz, A., Luettich, K., Frentzel, S., et al., 2020. In vitro high-content imaging-based phenotypic analysis of bronchial 3D organotypic air–liquid interface cultures. SLAS Technology: Translating Life Sciences Innovation 247263031989547. https://doi.org/10.1177/2472630319895473.

Meiners, S., Eickelberg, O., Königshoff, M., 2015. Hallmarks of the ageing lung. Eur. Respir. J. 45, 807–827. https://doi.org/10.1183/09031936.00186914.

Müller, L., Brighton, L.E., Carson, J.L., Fischer, W.A., Jaspers, I., 2013. Culturing of human nasal epithelial cells at the air liquid interface. J. Vis. Exp. 50646. https://doi.org/10.3791/50646.

Omiecinski, C.J., Vanden Heuvel, J.P., Perdew, G.H., Peters, J.M., 2011. Xenobiotic metabolism, disposition, and regulation by receptors: from biochemical phenomenon to predictors of major toxicities. Toxicol. Sci. 120, S49–S75. https://doi.org/10.1093/toxsci/kfq338.

Pezzulo, A.A., Starner, T.D., Scheetz, T.E., Traver, G.L., Tilley, A.E., Harvey, B.-G., et al., 2011. The air-liquid interface and use of primary cell cultures are important to recapitulate the transcriptional profile of in vivo airway epithelia. Am. J. Phys. Lung Cell. Mol. Phys. 300, L25–L31. https://doi.org/10.1152/ajplung.00256.2010.

Pirkle, J.L., Wolfe, W.H., Patterson, D.G., Needham, L.L., Michalek, J.E., Miner, J.C., et al., 1989. Estimates of the half-life of 2,3,7,8-tetrachlorodibenzo- *p* -dioxin in Vietnam veterans of operation ranch hand. J. Toxicol. Environ. Health 27, 165–171. https://doi.org/10.1080/15287398909531288.

Powles-Glover, N., 2014. Cilia and ciliopathies: classic examples linking phenotype and genotype—an overview. Reprod. Toxicol. 48, 98–105. https://doi.org/10.1016/j.reprotox.2014.05.005.

Ramadoss, P., Marcus, C., Perdew, G.H., 2005. Role of the aryl hydrocarbon receptor in drug metabolism. Expert Opin. Drug Metab. Toxicol. 1, 9–21. https://doi.org/10.1517/17425255.1.1.9.

Schmidt, H., Michel, C., Braubach, P., Fauler, M., Neubauer, D., Thompson, K.E., et al., 2017. Water permeability adjusts resorption in lung epithelia to increased apical surface liquid volumes. Am. J. Respir. Cell Mol. Biol. 56, 372–382. https://doi.org/10.1165/rcmb.2016-0161OC.

Schneider, D., Ganesan, S., Comstock, A.T., Meldrum, C.A., Mahidhara, R., Goldsmith, A.M., et al., 2010. Increased cytokine response of rhinovirus-infected airway epithelial cells in chronic obstructive pulmonary disease. Am. J. Respir. Crit. Care Med. 182, 332–340. https://doi.org/10.1164/rccm.200911-1673OC.

Tarran, R., Button, B., Picher, M., Paradiso, A.M., Ribeiro, C.M., Lazarowski, E.R., et al., 2005. Normal and cystic fibrosis airway surface liquid homeostasis: *the effects of phasic shear stress and viral infections*. J. Biol. Chem. 280, 35751–35759. https://doi.org/10.1074/jbc.M505832200.

Tosoni, K., Cassidy, D., Kerr, B., Land, S.C., Mehta, A., 2016. Using drugs to probe the variability of trans-epithelial airway resistance. PLoS One 11, e0149550. https://doi.org/10.1371/journal.pone.0149550.

Tsartsali, L., Hislop, A.A., McKay, K., James, A.L., Elliot, J., Zhu, J., et al., 2011. Development of the bronchial epithelial reticular basement membrane: relationship to epithelial height and age. Thorax 66, 280–285. https://doi.org/10.1136/thx.2010.149799.

Wilkinson, K.E., Palmberg, L., Witasp, E., Kupczyk, M., Feliu, N., Gerde, P., et al., 2011. Solution-engineered palladium nanoparticles: model for health effect studies of automotive particulate pollution. ACS Nano 5, 5312–5324. https://doi.org/10.1021/nn1032664.